ERRA-BALSELLS Rosa (Orcid ID: 0000-0003-0169-0173)

norHarmane containing ionic liquid matrices for low molecular weight MALDI-MS carbohydrate analysis: The perfect couple with α-cyano-4-hydroxycinnamic acid

Tobías Schmidt De León[1,2], María L. Salum[1,2] and Rosa Erra-Balsells[1,2]*

[1]Universidad de Buenos Aires. Facultad de Ciencias Exactas y Naturales. Departamento de Química Orgánica. Pabellón II, 3er P., Ciudad Universitaria, 1428 Buenos Aires, Argentina.

[2] CONICET, Universidad de Buenos Aires. Centro de Investigación en Hidratos de Carbono (CIHIDECAR). Facultad de Ciencias Exactas y Naturales Pabellón II, 3er P. Ciudad Universitaria, 1428 Buenos Aires, Argentina.

Keywords: MALDI-MS; CHCA.nHo; IL MALDI matrix; LMW carbohydrates; LMW neutral carbohydrates; LMW sulfated carbohydrates,

*Corresponding Author: Rosa Erra-Balsells. Fax/Phone: +54-1145763346. E-mail: erra@qo.fcen.uba.ar.

This article has been accepted for publication and undergone full peer review but has not been through the copyediting, typesetting, pagination and proofreading process which may lead to differences between this version and the Version of Record. Please cite this article as doi: 10.1002/jms.4375

Abstract

Cinnamic acid derivatives, particularly α-cyano-4-hydroxycinnamic acid (*E*-α-cyano-4-hydroxycinnamic acid or (*E*)-2-cyano-3-(4-hydroxyphenyl)prop-2-enoate; CHCA) has been extensively used especially for protein and peptide analysis. Together with the introduction of ionic liquid MALDI matrix (ILM) started the study of applications of IL prepared with CHCA and a counter organic base (i.e., aliphatic amines) in which CHCA moiety is the chromophore responsible of UV-laser absorption. Although the extensive studies of norharmane (9*H*-pyrido[3,4-*b*]indole; nHo) applications as matrix and its peculiar basic properties in the ground and electronic excited state, it was never tested nHo containing ILM in MALDI-MS experiments. This pyrido-indole compound was introduced as MALDI matrix twenty two years ago for different applications including low molecular weight (LMW) carbohydrates (neutral, acidic and basic carbohydrates). These facts encouraged us to use it as a base, for the first time, for ILM preparation. As a rational design of new IL MALDI matrices, *E*-α-cyanocinnamic acid.nHo and *E*-cinnamic acid.nHo were prepared and their properties as matrices studied. Their performance was compared with that of (i) the corresponding IL prepared with butylamine as basic component, (ii) the corresponding crystalline *E*-α-cyanocinnamic and *E*-cinnamic acid and (iii) the classical crystalline matrices (2,5-dihydroxybenzoic acid, DHB; nHo) used in the analysis of neutral/sulfated carbohydrates. The IL DHB.nHo was tested too. Herein we demonstrate the outstanding performance for the IL CHCA.nHo for LMW carbohydrate in positive and negative ion mode (linear and reflectron modes). Sulfated oligosaccharides were detected in negative ion mode and although the dissociation of sulfate groups was not completely suppressed the relative intensity (RI) of $[M\text{-}Na]^-$ peak was quite high. Additionally, to better understand the quite different performance of each IL tested as matrix the physical and morphological properties in solid state were studied (optical image; MS image).

1. Introduction

Since their introduction as matrices at the beginning of matrix-assisted UV laser desorption/ionization mass spectrometry (MALDI-MS) development, cinnamic acid derivatives, particularly α-cyano-4-hydroxycinnamic acid ((*E*)-2-cyano-3-(4-hydroxyphenyl)prop-2-enoate; CHCA) [1] has been extensively used especially for protein and peptide analysis. As CHCA has been successfully used, efforts to prepare new compounds rationally designed keeping the α-cyanocinnamic core structure have been made. Thus, the synthesis and applications of *E*-α-cyano-4-chlorocinnamic acid (4ClCHCA) [2], *E*-α-cyano-4-fluorocinnamic acid (4FCHCA) [2], *E*-2-cyano-3-(naphthalene-2-yl)acrylic acid [3], *E*-3-(anthracen-9-yl)-2-cyanoprop-2enoic acid [3] and other CHCA halo-derivatives (4-bromo and different combinations of poly fluoro-, poly-chloro-fluoro-phenyl-α-cyanocinnamic acids) [4], have been described. These compounds are called "second generation matrix" [4].

Together with the introduction of ionic liquid (IL) MALDI matrix (ILM) [5] started the study of applications of IL prepared with CHCA and a counter organic base (e.g., butylamine, tributylamine, tryethylamine, pyridine, 3-aminoquinoline, 1-methylimidazole, aniline, 1,1,3,3-tetramethylguanidine, just to name a few) [6, 7], in which CHCA moiety is the chromophore responsible of UV-laser absorption.

Although the extensive studies of norharmane (nHo) applications as matrix and its peculiar basic properties, it was never tested nHo containing ILM in MALDI-MS experiments. This 9*H*-pyrido[3,4-*b*]indole compound, member of the family of β-carboline alkaloids, was introduced as MALDI matrix twenty two years ago for different applications including neutral, acidic and basic carbohydrates and proteins in positive and negative ion modes [8, 9, 10], sulfated polysaccharides [11, 12], sulfoglycosphingolipids [13], lipids [14] and polymers

[15, 16] in negative ion mode. Recently, nHo has successfully applied in MALDI-MS imaging (MALDI-MSI) for lipid profiles in animal tissues (e.g., phospholipids distribution in brain tissue [17], lipids in tumor [18], among others). The special acid-basic properties shown by nHo in the ground and electronic excited state (pKa = 7.2-7.9 in the ground state [15, 19] and pKa* = 13.0-14.7 in the electronic excited singlet (S_1) state [20]) encouraged us to use it as a base, for the first time, for ILM preparation.

In the present paper, neutral and sulfated carbohydrates were chosen as analytes because we are interested in development of new matrices for sugar analysis, especially for low molecular weight (LMW) carbohydrates [21, 22]. As it is known classic MALDI cinnamic acid matrices (i.e, *E*-3,5-dimethoxy-4-hydroxycinnamic acid, SA; *E*-3-methoxy-4-hydroxycinnamic acid, ferulic acid, FA, and CHCA too, do not perform well in carbohydrate analysis [23].

LMW compounds constitute a family with a common inconvenience in MALDI-MS analysis. The region of their m/z values is the region where classical crystalline matrices show not only the molecular ions but abundant signals with different origin (i.e, fragments from molecular ions; clusters; fragments from clusters) too. The different efforts conducted in order to overcome this experimental problem are described in detail in the recent Calvano's review [24]. The same topic is also discussed in U. Bahr and T. W. Jaskolla review on Employing 'Second Generation' Matrices [4]. In the case of CHCA several matrix-related ions are generated together with sodiated and potassiated adducts covering the m/z range up to 1300 (e.g., m/z 1287 ($[5M+4K-3H]^+$) [24]).

MALDI-MS analysis of sulfated oligosaccharides is problematic because labile sulfate groups are frequently dissociated (in source decomposition, ISD) and thus ion species of intact molecules are hardly detected [23, 25]. Among commercial cinnamics, SA was checked for sulfated carbohydrates but the presence of abundant matrix ions in the region of

the molecular ion interfered with detection [26]. Methods such as stabilizing by derivatization of sulfate groups [23, 25] and development of cool matrices such as 2,5-dihydroxybenzoic acid (gentisic acid, DHB) and ionic liquid matrices [25, 27, 28] have been reported. DHB is a cool matrix widely used for carbohydrate analysis. A weak point of DHB is the formation of inhomogeneous needle-shaped crystals, and therefore the analytes are ionized in only a few small areas on the probe called sweet spots. On the contrary, nHo as matrix provides abundant homogeneously distributed sweet spots all over the sample but behaves as a hotter matrix than DHB in similar experiments [28].

In the present paper we studied the CHCA.nHo IL as matrix for LMW carbohydrate analysis and compared with nHo, CHCA and with CHCA.BAM (butylamine, BAM), a CHCA containing ILM previously applied to low molecular weight carbohydrate analysis [5, 7].

DHB was used as crystalline reference matrix. Furthermore, DHB included in IL with nHo (DHB.nHo) and BAM (DHB.BAM) were included in the study too. SA, SA.nHo and SA.BAM have been also included for comparison because this cinnamic acid as SA.BAM ILM has been previously checked [7]. Two commercially available 4-haloderivatives of *E*-α-cyanocinnamic acid, *E*-4-chloro-α-cyanocinnamic acid (4ClCHCA) [2], *E*-4-fluoro-α-cyanocinnamic acid (4FCHCA) [2] and the ILs 4ClCHCA.nHo and 4FCHCA.nHo were checked as well as 4ClCHCA.BAM and 4FCHCA.BAM. The application of 4ClCHCA.BAM as matrix has been described by Towers et al [29, 30].

For the description of the study we focused our attention on CHCA and the results obtained from comparative experiments (linear, reflectron and MS/MS modes) with the other compounds applied as matrices are discussed too. Physical and morphological properties (optical image) of crystalline matrix and its ILs as well as the homogeneity of the sweet spots distribution all over de analyte-matrix sample were compared. Furthermore, comparative UV-

absorption spectra with different chromophore concentration (e.g., 20 μM and 20 mM) and in solid state were conducted and here discussed.

2. Materials and Methods

2.1. Chemicals and Material

The β-carboline 9*H*-pyrido[3,4-*b*]indole (*nor*-harmane, nHo), 2,5-dihydroxybenzoic acid (DHB), the *E*-cinnamic acids (4-hydroxy-a-cyanocinnamic acid or *E*-4-hydroxy-a-cyanocinnamic acid (CHCA), *E*-4-chloro-α-cyanocinnamic acid (4ClCHCA), *E*-4-fluoro-α-cyanocinnamic acid (4FCHCA), *E*-3,5-dimethoxy-4-hydroxycinnamic acid, SA) and butylamine (BAM) were purchased from Aldrich (USA). The general structure of these compounds are shown in Scheme S1 (supplementary information). Ionic Liquids matrices were prepared by dissolving 0.3-0.1 g of acid in 10-5 mL of methanol, adding subsequently an equimolar amount of the organic base (BAM; nHo) and keeping the mixture under sonication for 10 min. Then, solvent was evaporated using a vacuum evaporator. The residue obtained (solid powder) was kept in the dark at room temperature for characterization (melting point (m.p.), UV-visible absorption and UV-visible diffuse reflectance apectroscopy and ^{1}H NMR spectroscopy).

The sulfated neocarrabiose oligosaccharides (neocarratetraose 4^{1},4^{3}-disulfate disodium salt (NCT) was purchased form Sigma-Aldrich (USA). Glucose (Glc), maltotetraose (M4), maltopentaose (M5), maltohexaose (M6), maltoheptaose (M7), the thiosaccharide isopropyl-β-D-1-thiogalactoside (IPSG) and the cylic maltoses (β-ciclodextrin (bCD), heptakis(*O*-methyl)-β-cyclodextrin (MbC), heptakis(2,6-di-*O*-methyl)-β-cyclodextrin (DMbCD), heptakis(2,3,6-tri-*O*-methyl)-β-cyclodextrin (TMbCD), and heptakis(2-hydroxypropil)-β-cyclodextrin ((OHP)bCD) were obtained from Sigma Chemical, Tokyo, Japan. Fructans (fructose (F1), sucrose (F2), 1-kestose (F3), nystose (F4) and 1^{F}-fructofuranosylnystose (F5))

were obtained from Wako Pure Chemical Industries, Japan. The general structures of the studied carbohydrates are shown in Scheme S1 (supplementary material). All the organic solvents (J. T. Baker HPLC grade) were used as purchased without further purification. Water of very low conductivity (Milli-Q grade) was used.

2.2. Sample Preparation

Matrix stock solutions were made as follows: (i) classical matrix: by dissolving 2 mg of the selected compound in 1 mL of methanol/water (65:35. v/v) (concentration aprox. 0.01 M) and (ii) ionic liquid matrix (ILM): by dissolving the acid in methanol/water (65:35. v/v) to get a 0.005 M solution and subsequently adding the necessary amount of the base to get an equimolar base solution (acid to base ratio 1:1; mol/mol); ILM solutions with 0.01 M concentration of each IL component were also prepared. Analyte solutions were freshly prepared by dissolving the carbohydrate (1 mg) in water (1 mL).

To prepare the analyte-matrix sample the thin-film layer method (sandwich method) [8] was used. Typically 0.5 µL of the matrix solution was placed on the target plate and air-dried at room temperature. Subsequently, 0.5 µL of the analyte solution was placed on the target plate covering the matrix and partially dissolving it and air-dried. Then, two additional portions (0.5 µL) of matrix solution were deposited on the same target plate, producing a partial dissolution of the previously deposited thin-film. The matrix to analyte ratio was 3:1 (v/v) and the matrix and analyte solution loading sequence was: (i) matrix, (ii) analyte, (iii) matrix, and (iv) matrix.

Comparative experiments were also conducted preparing the analyte-matrix sample by the mixture method. The pre-prepared mixture was done mixing the matrix and analyte solutions in a 3:1 (v/v) ratio. Two portions (0.5 µL) of the mixture were successively loaded on the

target plate and air-dried at room temperature. Similar results were obtained with both sample preparation methods.

2.3. Limit of Detection (LOD)

As example of neutral carbohydrate, bCD was chosen for the determination and comparison of the experimental limit of detection (LOD) achievable with CHCA, nHo, CHCA.BAM and CHCA.nHo, in positive ion mode. Serial dilutions of an aqueous stock solution of the carbohydrate (10 mM) with water were carried out and analyzed. The lowest concentration tested was 0.1 μM. A 0.5 μL aliquot of the analyte solution was spotted on a dry layer prepared with 0.5 μL of matrix solution following the general method for sample preparation described above. The monitoring ion was $[M+Na]^+$ ($[bCD+Na]^+$). Similar LOD experiments were conducted in negative ion mode using stock aqueous NCT solution (10 mM) successively diluted with water. The lowest concentration tested was 0.1 μM. The ion monitored was $[M-Na]^-$ ($[NCT–Na]^-$). LOD was defined as the pmol of analyte (bCD or NCT) transferred on the target plate which yielded a signal to noise ratio (S/N) that was S/N $\geq$ 4 (Table 1).

2.4. Signal Stability

To assess the signal stability and longevity of the liquid matrices 100 spectra were acquired from a central position of a liquid droplet containing 100 fmol of the analyte. Each spectrum was acquired as the sum of 100 single-shot spectra at 50 Hz with a gap of ~1 s between each acquisition, resulting in a total of 10 000 individual exposures on a single position.

2.5. MALDI Mass Spectrometry Experiments

Spectra were recorded on a Bruker Ultraflex II TOF/TOF, controlled by the FlexControl 3.0 software (Bruker Daltonics, Bremen, Germany). Desorption/Ionization was performed using a frequency tripled Nd:YAG laser emitting at 355 nm with a 100 Hz shot frequency. All mass spectra described were taken in linear and reflectron modes. Experiments were performed using firstly the full range setting for laser firing position in order to select the optimal position for data collection, and secondly fixing the laser firing position in the sample sweet spots. The laser power for each analyte was adjusted to obtain: high signal-to-noise ratio (S/N), minimal fragmentation of the parent ion and good resolution for the matrix that required the highest volatilization/ionization threshold power; this matrix was in all the cases nHo. This power (in general 20 %, see information in each figure caption), was fixed for the other matrices tested in the comparative experiments (see an example in Supplementary information, Figure S1v). Each mass spectrum was generated by averaging 200 lasers pulses per spot.

Selected examples were analyzed in positive and negative MS/MS mode (LIFT mode, laser power precursor ion 30% and for fragment ions 80%). Results were analyzed with the program FlexAnalysis, respectively. MTP 384 target plate steel T F was used (Part No.: 209519; target frame (# 74115); 384 circular spots, 3.5 mm diameter; S/N 03630).

2.6. UV-visible absorption and diffuse reflectance spectroscopy

UV-visible absorption spectra of the matrix (crystalline and ILM) in methanol, methanol:water (65:35) and acetonitrile solutions were recorded on a Shimadzu UV-1203

spectrophotometer. Concentrations used were 10^{-5} to 10^{-3} M (i.e., 20 μM and 1 mM). Measurements were made in quartz cells of 1 cm optical-path length (Hellma, Germany). Diffuse reflectance measurements with solid samples were performed by means of a spectrophotometer (UV3101PC, Shimadzu) equipped with an integrating sphere (ISR-3100; Shimadzu). Barium sulfate was used as a white reference standard to adjust 100% reflectance level.

2.7. MALDI Imaging

The homogeneity of the MALDI sample preparation for each of the matrices (CHCA, DHB, SA; nHo; CHCA.nHo, CHCA.BAM, DHB.nHo, DHB.BAM, SA.nHo and SA.BAM) was assessed by MALDI imaging. The on-target sample amounts deposited was 0.5 uL of bCD solution (aprox. 100 fmol bCD). Samples were prepared according to the general sample preparation method described above. Both concentration of ILM (0.005 and 0.01 M) were checked (see Figures 4 and S4).

Custom geometry files defining sampling positions were created adapted to the geometry of the type of target plate used. For each round spot containing the sample, the minimum square containing it was defined .and divided in a 10x10 set of squares as the number/location of positions to sample. The positions were sampled manually. Spectra were acquired by data accumulation from a total of 200 laser pulses at each position. The resulting spectral files were combined and the peak intensity for a user defined mass ($[bCD+Na]^+$ for each position was exported to OriginPro 8 using another in-house-written program to create two-dimensional ion-density maps. Normalization of peak intensity and adjustment of color scale was also performed using this software. Here, we mentioned that comparisons among MS

images are semi-quantitative because each signal value was derived from the relative intensity normalized by the highest intensity spot on the figure.

3. Results and Discussion

The rationale of the approach followed here was to synthesize ionic liquid matrices (ILMs) candidates keeping in the anionic structure the α-cyanocinnamic moiety (Ar-C=C(CN)-COOH) of the α-cyanocinnamic acid core, with different nature and positions of the substituents attached to the phenyl group (Ph), and to introduce the use of nHo as the basic moiety (Scheme S1). Taking into account the UV-visible absorption spectra of the acid-base pair containing these ILs, in the present study both ILM moieties absorb individually at 355 nm (see below).

3.1. *Characteristics of the investigated matrices*

Physical properties (m.p., UV-absorption spectra and ^{1}H-NMR spectra) for characterization of ILMs were checked. Here is important to note that (i) in all cases the m.p. of the acid.nHo IL is lower than that of the acid (e.g., CHCA 245-250 ^{O}C [31]; CHCA.nHo 165-166 ^{O}C) and of nHo (235-238 ^{O}C [32]); (ii) The ^{1}H-NMR spectra for the IL cinnamic acid.nHo show the shielding of the nHo proton signals to higher δ values (Δδ aprox +2-3 ppm) in agreement with the cationic character of the nHo moiety (protonation of the pyridinic nitrogen) (e.g. Figures S1i and S1ii, ^{1}H-NMR spectra, nHo, CHCA and CHCA.nHo), and (iii) The UV-visible absorption spectra in methanol solution for the CHCA, nHo and CHCA.nHo (Figure 1a), show that the spectrum of the IL CHCA.nHo is quite similar in the 300-400 nm region to

that of CHCA (ε(355 nm) in methanol; 1.45 x 10^4 and 1.19 x 10^4 respectively). The higher ε values shown for CHCA in this region compared with that of nHo explains this experimental fact (ε(355 nm) in methanol; 1.19 x 10^4 and 2.59 x 10^3 respectively). As BAM has been used previously to prepare IL matrix and particularly CHCA.BAM IL [5, 7, 30, 31] this amine has been included in the present study as well as the crystalline matrix DHB and SA (see in supplementary material: Figure S1iii, DHB, DHB.BAM, and DHB.nHo; SA, SA.BAM and SA.nHo; 4ClCHCA, 4ClCHCA.BAM and 4ClCHC.nHo; 4FCHCA, 4FCHCA.BAM and 4FCHC.nHo UV-visible absorption spectra). The corresponding λmax and ε in methanol, as well as ε at λ=355 nm are included in Table S1. These UV-visible absorption data have been got from 10^{-5} M methanolic solutions (Beer – Lambert conditions) [33, 34]. UV-visible absorption spectra were also acquired increasing matrix concentration, beyond the Beer-Lambert conditions [33, 34] and also in solid-state as diffuse reflectance UV-visible spectra (Figures 1a-c). The CHCA and CHCA.nHo bands were getting wider showing the latter a bathochromic shift (red shift). At higher concentration (10^{-3} M) and in solid state CHCA, nHo and CHCA.nHo absorb efficiently at longer wavelengths including 355 nm (Figure 1c). Although CHCA.BAM showed some hypsochromic effect (shifting to shorter wavelength) the absorbance at 355 nm is quite important (Figures 1a-c). The hypsochromic effect of aliphatic amines on the UV-Absorption spectra (λmax) of cinnamic MALDI matrix was discussed elsewhere [35]. Similar bathochromic effect was observed for the other nHo containing IL matrix (Figure S1iii). For morphological inspection (optical image) of the solid matrix deposited on the target plate the dried droplet method was used to prepare the sample. Fresh matrix solution was prepared in methanol/water as detailed in Materials and Methods (Experimental). As a result, CHCA gave small crystals distributed at random, as aggregates, all over the sample surface (Figure 1e) and nHo showed the aspect of abundant needles covering all the spot surface solid (Figure 1d).When the ILM CHCA.nHo was deposited on

the target plate showed the aspect of a solid solution (glass) (Figure 1g). This optical homogeneity observed matched with the higher homogeneous analyte distribution in the IL matrix-analyte sample observed during data acquisition experiments (see below). Digital images were registered on the Bruker Ultraflex II TOF/TOF. Additional images for the other matrices tested are included in Figure S1iv (supplementary material).

3.2. *MALDI mass spectrometry analysis*

3.2.1. *IL Matrices*

Laser desorption / ionization (LDI) experiments were conducted with the 355 nm laser on the Bruker Ultraflex II TOF/TOF in positive and negative ion modes. Experiments were run in the same conditions (solution concentration; solvent; volume loaded on the target plate; experimental parameter; etc.). In both ion modes the laser power applied was similar to that used in experiments conducted for carbohydrate analysis (see section 2.5. MALDI Mass Spectrometry Experiments, and Figure S1v), Briefly, results obtained are as follows. CHCA always showed, in positive ion mode, more abundant peaks (molecular ion, fragments and clusters) than nHo and called our attention that CHCA.nHo only showed the signal corresponding to $[nHo+H]^+$ without any of the typical clusters shown by CHCA. In negative ion mode the spectra of nHo and CHCA.nHo were quite simple. nHo showed only the $[nHo-H]^-$ species at *m/z* 167 and CHCA.nHo showed one signal at *m/z* 188 corresponding to $[CHCA-H]^-$. This $[M-H]^-$ species and the $[M-CO_2-H]^-$ fragment at *m/z* 144 were observed in the spectrum of CHCA together with quite intense cluster signal at *m/z* 779, *m/z* 815 and 968 (not assigned). On the contrary of the result observed for CHCA.nHo, in the 4ClCHCA.nHo and 4FCHCA.nHo the presence of nHo did not produce a clear cleaning effect on the corresponding LDI mas spectra. Furthermore, in positive ion mode CHCA.BAM showed

higher amount of cluster signals than CHCA.nHo. For comparison in supplementary material are included and commented the LDI spectra mentioned above (Figures S1vi-i to S1vi-iv).

3.2.2. *Neutral carbohydrates*

To begin with our comparative study of the application of IL constituted by α-cianocinnamic acid and nHo as MALDI matrix for analysis of carbohydrates, its performances as matrix for commercially available carbohydrates fructans, maltoses, thiosaccharides, cyclodextrins, subtituted cyclodextrins and sulfated sugars were investigated (analytes are listed in section 2. Materials and Methods; general molecular structure of the compounds studied are included in Scheme S2, supplementary material).

As an example, in Figure 2 the spectra obtained in positive ion mode by deposition of solution of β–cyclodextrin (bCD) on air-dried layers of the examined matrix (sandwich method) are shown (monitored ion $[M+Na]^+$). We used bCD aqueous solution without any salt added (not salt doped). Experiments were conducted in linear and reflectron positive ionization mode. The efficiency of the desorption/ionization of each carbohydrate as mono-sodiated species ($[bCD+Na]^+$) as well as the clusters observed depend on the compound used as matrix., i.e., nHo (Figure 2a), CHCA (Figure 2b) and CHCA.nHo (Figure 2d). For comparison, the IL CHCA.BAM, has been also checked in the same experiment because its application for LMW carbohydrate analysis has been previously described [7] (Figure 2c). Besides, DHB a popular carbohydrate crystalline acidic matrix [36] has been used for comparison used as DHB (Figure 2e), IL DHB.BAM and IL DHB.nHo (Figures 2f and 2g).

The IL CHCA.nHo shown to be better matrix than CHCA and nHo as well as DHB and DHB.nHo. This IL matrix yielded higher intensity intact molecular species as $[M+Na]^+$ being the absolute intensity value higher than that expected as individual desorption/ionization process produced by CHCA and nHo separately. Thus, a mutual beneficial cooperative effect

between CHCA and nHo should be operating (photo and/or thermal effect). In the particular case of DHB the presence of nHo in the IL DHB.nHo did not show a clear effect on its matrix performance; $[bCD+Na]^+$ intensity remains quite similar in both cases. As can be seen in Figures 2c and 2d the efficiency of both ILM CHCA.nHo and CHCA.BAM are quite good, and particularly for bCD and some other low molecular carbohydrate studied they are both quite efficient ILM, outperforming the solid crystalline matrices. Both organic base compounds have pKa around 10; BAM pKa = 10.6 [7], nHo pKa(N) (nitrogen at position 2 in pyridinic moiety) = 7.2-7.9 [15, 19] and nHo pKa(NH) = 14.5 (nitrogen at 9 ring position in indolic moiety) [18]. Furthermore, nHo in its electronic excited singlet state (S1) has a pKa* = 13-14.7 [15, 19, 20]. The corresponding reflectron spectra are included in the same figure (Figures 2h to 2n) showing a similar trend than the above described for the linear mode.

When the other neutral maltoses, thiosacchrides, and fructans were studied always CHCA.nHo performed as quite good matrix in both modes (linear and reflectron) and sometimes CHCA.BAM was superior (see as examples M7, M6, M5 and F5 in Figure S2i, and IPSG, F2 and M4 in Figures S2ii-S2iii, in supplementary material). As an exception, for Glc the experimental conditions (sample preparation, laser power, etc.) to diminish the clusters signals could not be found (Figure S2ii, left column) but in reflectron mode CHCA.nHo was the best. As examples the spectra obtained in reflectron mode for the thiosaccharide isopropyl-β-D-1-thiogalactoside (IPSG) and the fructan sucrose (F2) with nHo, CHCA and CHCA.nHo are shown in Figure 3. Besides, among this carbohydrate group we selected bCD, M7 and M5 to conduct MS/MS experiments in order to compare the behaviour as matrix of nHo, CHCA and CHC.nHo. CHCA.nHo showed to be again the more efficient matrix in these experiments (Figures S2iv-vi). The typical carbohydrate fragmentation patters were observed (e.g., $[M+Na-(162)_{n=1-6}]$ for bCD, and M7; $[M+Na-(162)_{n=1-4}]$ for M5; $[M+Na-18-(162)_{n=1-6}]$ for M7 and $[M+Na-18-(162)_{n=1-4}]$ for M5, and $[M+Na-60-(162)_{n=1-3}]$

for M5. Furthermore, some commercial substituted b-cyclodextrins (MbCD, DMbCD, TMbCD and (HOPb)CD; see formulas in Scheme S2) were selected as more complex samples. As an example spectra obtained for (HOP)bCD with nHo, CHCA and CHCA.nHo are shown in Figure 3 (reflectron mode) and Figure S3i (linear and reflectron modes). Although m.w. of the mono-hydroxypropil-β-clyclodextin is 1192 Da ($[M+Na]^+$ *m/z* = 1215) the commercial product is a mixture of poly-hydroxypropil-β-cyclodextins with formula (HOP_nbCD with n=1-9 (Figure 3, m/z at 1215, 1273, 1331, 1389, 1447, 1505, 1563, 1621 and 1679). Furthermore, spectra for MbCD, DMbCD and TMbCD are also included in supplementary information (Figures S3ii-iv); they showed to be complex mixtures with the formula $(CH3)_{9\text{-}16}$bCD, $(CH3)_{13\text{-}18}$bCD and $(CH3)_{20\text{-}21}$bCD respectively. Best results were obtained with the IL CHCA.nHo as matrix. In all cases abundant sweet spots were easy to find, homogenously distributed all over the sample surface for CHCA.nHo while they were more difficult to find for the other matrices. In Figures 4a-d the spot surface intensity maps (image) showing the intensity of the $[bCD+Na]^+$ signal obtained comparing several matrices are shown. Higher intensity signals, homogeneously distributed, were obtained when IL CHCA.nHo was used (Figure 4d). Performances were quite good with IL matrix 0.01-0.02 M solutions. Homogeneity shown by IL CHCA.nHo was higher than that shown by CHCA.BAM (Figures 4c and d). For IL matrices containing DHB, DHB.BAM (Figures S4b and c) and DHB.nHo (Figure S4d), DHB.BAM showed analyte intensity signals lower than those from crystalline matrices nHo and DHB (Figures S4a and b) and also from IL DHB.nHo (Figure S4d), DHB.nHo performed far better than DHB.BAM and crystalline DHB but crystalline nHo matrix was the best. The effect of BAM and nHo on the properties of the ILM SA.BAM and SA.nHo is quite similar than those described for DHB (Figures S4e-g).

Results quite interesting were obtained with the other α-cyanocinnamic acids studied as crystalline and as containing ILM. As is summarized in Figure 5 the results obtained when bCD and M7 were examined showed that although 4ClCHCA is not a good matrix at all for these pair of LMW carbohydrates and nHo performance is quite good, the resulting ILM 4ClCHCA.nHo yielded intact molecular ions as $[M+Na]^+$ species with intensity almost two times higher than the produced by crystalline nHo (molar concentration of nHo solution and 4ClCHCA.nHo solution was the same). Undoubtedly the mutual effect on photo and thermal individual properties of the components of this ILM when they are operating together would be the reason of this so drastic performance change. These spectra in detail are shown in Figures S5a-S5d (supplementary material). As can be seen in these figures, the IL 4ClCHCA.BAM showed a worse behavior than crystalline 4ClCHCA. Previously 4ClCHCA containing ILM, combining 4ClCHCA and 3-aminoquinoline (3-AQ) has been described as efficient matrix for protein and peptide analysis [29, 30]. On the contrary, as can be seen in Figure 5 and Figures S5e-g, 4FCHCA showed a poor behavior as matrix not improved much as IL 4FCHCA.BAM and, although improved a bit, showed minor efficiency as IL 4FCHCA.nHo than crystalline nHo. In this case the mutual photo and/or thermal effect is not cooperative at all, and 4FCHCA quenches nHo properties as MALDI matrix. The trend of results obtained was similar for M7 when the same family of crystalline and ILM were used (see normalized relative intensity of $[M7+Na]^+$ species in Figure 5 and Figures S5h-n).

3.2.3. *Sulfated carbohydrates*

Sulfated oligosaccharide MALDI-MS analyses were conducted in both ion modes, in linear and reflectron modes. Best results were obtained in negative ion mode. As an example, in Figure 6 the spectra obtained in negative ion mode for neocarratetraose $4^1,4^3$-disulfate disodium salt (NCT; m.w. 834.62; general molecular structure for sulfated carbohydrates is

included in Scheme S2, supplementary material) with three different matrices are displayed. Thus, the application of the CHCA, nHo and CHCA.nHo for sulfated oligosaccharides demonstrated that CHCA.nHo showed good performance in terms of sensitivity higher than crystalline nHo, and both behaved better than crystalline CHCA, in negative ion mode. When CHCA was used, intact molecular ion as $[M\text{-}Na]^-$ was detected as a lower intensity signal and the corresponding main fragment at m/z 709 (see bellow, fragment 1) was not detected or just as very minor signal. On the contrary, important matrix-cluster-signal at *m/z* 799 was detected (* = cluster). The fragmentation in negative ion mode mainly occurred by dissociation of the sulfate groups according a loss of 102 Da from the $[M\text{-}Na]^-$ to yield $[M\text{-}Na\text{-}nSO_3Na+nH]^-$ (i.e., Frag. 1 = $[M\text{-}Na\text{-}SO_3Na+H]^-$) (see in Figure 6, fragment 1 at *m/z* = 709 and in Figures S6i and S6ii) [27, 28]. Additional figures comparing the spectra obtained for NCT using 4ClCHCA and 4FCHCA and the corresponding ILMs with nHo, 4ClCHCA.nHo and 4FCHCA.nHo, as matrix are included in supplementary material (Figures S6i and S6ii; laser power 20% and 40% respectively). In the case of 4FCHCA the $[NCT\text{-}Na]^-$ intact molecular ion signal was not observed (Figures S6i(e) and S6ii(e)). On the contrary 4ClCHC and 4ClCHC.nHo ahowed a different behaviour as matrix (Figures S6i(a-d) and S6ii(a-d)) Alhoutgh the signal intensity of the $[NCT\text{-}Na]^-$ peak are quite similar in the spectrum when crystalline nHo and 4ClCHC.nHo were used, the relative intensity of the signal at *m/z* 709 (assigned to NCT fragment 1) in the latter drastically diminished, behaving the IL as a cooler matrix than nHo did. Besides, 4ClCHCA did not induce desorption/ionizaiton by itself as MALDI matrix (analyte signals were not detected when it was the matrix; Figures 6i(b) and 6ii(b)). Then for NCT MALDI analysis at laser power 20% the IL 4ClCHCA.nHo showed minor efficiency than nHo while at laser power 40% showed an efficiency similar to nHo. Altought this fact the IL 4ClCHCA.nHo behaved as a cooler matrix than nHo, showing 4ClCHCA a benefitial "cooling" effect on nHo as matrix for

sulfated sugars in negative ion mode (Figures S6i(a), S6i(d), S6ii(a) and S6ii(d)). In all the comparative experiments CHCA.nHo behaved as the best. Briefly, the comparative results expressed as normalized intensity of the $[NCT\text{-}Na]^-$ signal vs the IL used as matrix are summerized in Figures 7 and S7. Clearly the presence of 4ClCHCA in the 4ClCHCA.nHo IL seems to improve the behaviour of nHo as MALDI matrix (suppression of ISD). On the contrary the presence of 4FCHC seems to inhibite (quench) almost completely the cappability of nHo to work as matrix for NCT analysis in negative ion mode. In the case of CHCA clearly the eficience of CHCA.nHo is higher than that resulting of the simple summation (cooperative addition) of individual CHCA and nHo cappabilities of desorption/ionization NCT. The additional advantage was that all over the sample prepared with CHCA.nHo sweet spots were homogeneously distributed and easily to find.

3.2.4. *Dynamic range and limit of detection determination*

Dynamic range and limit of detection (LOD) studies for neutral sugars were conducted in positive ion mode. Table 1, shows the comparison between the results obtained for bCD deposited on the examined crystalline matrices CHCA and nHo, and the ILs CHCA.nHo and CHCA.BAM. The intensity of the mono-sodiated ion $[bCD+Na]^+$ in the positive ion mode was monitored. The dynamic ranges in which carbohydrate signal was detected with good signal/noise (S/N) ratios ($S/N \geq 4$) are listed. CHCA.nHo showed quite satisfactory LOD and dynamic range. Besides, the intensity of the signals was higher than those obtained with the other matrices (Figure 2). The results of examining the ratios of signal intensities to the concentrations of standard sugar (bCD) deposited on the matrix (Figures S8a and S8b), showed a remarkable concentration-sensitivity, especially in the case of CHCA.nHo. CHCA and nHo showed lower concentration-sensitivity. All matrices exhibited linearity. The intensity of the analyte signals yielded by CHCA.nHo were higher than those by CHCA and the lowest by nHo. In all the cases, intensity became practically independent of the carbohydrate concentration in the tested solution from bCD > 0.5 mg/mL (Figure S8a). Furthermore, with

increasing amount of carbohydrate deposited on CHCA (bCD > 1.0 mg/mL), the desorption/ionization (DI) efficiency of the carbohydrate decreased and the absolute intensity of the signal decreases instead of increases (Figure S8a).

Sulfated sugars were better detected (high ionization efficiency, good reproducibility, good S/N ratio) in negative ion mode as the species $[M-Na]^-$ (Figure 6). Thus, experiments were conducted in this ionization mode and the intensity of the ion $[M-Na]^-$ was monitored. As is shown in Table 1, LOD and dynamic range with CHCA.nHo for neocarratetraose 4,4'-disulfate disodium (NCT) was better than with CHCA.BAM and with nHo. Both, CHCA.BAM and nHo are good matrices and performed better than crystalline CHCA.

As a summary Table 1 shows the dynamic range and LOD obtained in both ion modes. Samples were not doped (no salt added) because higher intensity signals were observed in this experimental conditions.. CHCA.nHo, CHCA.BAM and nHo showed comparably satisfactory LODs and dynamic ranges for the neutral carbohydrates studied and they were superior to CHCA. In the negative ion mode CHCA.nHo and, CHCA.BAM performed better than nHo and CHCA was the worst. The superiority of the CHCA.nHo as matrix in both ion modes, probably originates because from the molecular contact-pair CHCA + nHo = CHCA.nHo = $[CHCA-H]^-.[nHo+H]^+$, a new structure/chromophore moiety is formed with photo-physical and/or thermal properties more suitable for the MALDI matrix role. Studies paying special attention on the thermal and photochemical properties of crystalline CHCA, crystalline nHo and the ILM CHCA.nHo as well as those of the other matrix here studied, are in progress in our laboratory.

Conclusions

Results obtained can be summarized as follows. (i) The new ionic liquid matrix (ILM) candidates with α-cyanocinnamic acid core and nHo as base, show quite different performance depending on the nature of the former. (ii) The presence of nHo improves CHCA.nHo LDI spectrum; Typical CHCA clusters, were not observed while for 4ClCHCA.nHo and 4FCHCA.nHo this "cleaning" effect was not operating. (iii) Morphological inspection (optical image) of the CHCA.nHo deposited on the target plate showed the aspect of a solid solution (glass) instead of the typical crystals of nHo and CHCA. (iv) The IL CHCA.nHo showed to be better matrix than CHCA and nHo as well as than DHB and SA. DHB performance was not improved at all including DHB in the IL DHB.nHo. Similar result was obtained with SA. (v) Although 4ClCHCA is not a good matrix for LMW carbohydrates (positive ion mode) the IL 4ClCHCA.nHo yielded intact molecular ions with RI almost two times higher than nHo. (vi) For sulfated sugars in negative mode, although the signal intensity of the $[M-Na]^-$ peaks were quite similar when nHo and 4ClCHCA.nHo were used, the relative intensity of the analyte fragments drastically diminished (suppression of ISD) in the latter, behaving the IL as a cooler matrix than nHo. On the contrary 4FCHCA in 4FCHCA.nHo quenches nHo properties as MALDI matrix.

The different mutual effect on the solid structure, and on the photo and/or thermal individual properties of the IL components would be the reason of these performances. The superiority of the IL CHCA.nHo probably originates because from the molecular contact-pair CHCA.nHo a new structure/ chromophore moiety is formed with photo-physical and/or thermal properties more suitable for the MALDI matrix role. The nature of the substituent in the aromatic group of α-cyanocinnamic acids seems to play an important role on the efficiency of the IL matrix here studied (α-cyano-4-HO-cinnamic acid > α-cyano-4-Cl-cinnamic acid >> α-cyano-4-F-cinnamic acid).

Finally, nHo is a commercial organic base quite stable in solution and in solid state (e.g., methanol solution can be kept at room temperature, under normal atmosphere, without any problem for several days and months; nHo solutions are not smelly at all). On the contrary, butylamine (BAM) is a colourless liquid organic base having the fishy-ammonia-like odor common to amines that acquires a yellow colour upon storage in air (oxidation-decomposition). Besides some BAM harmful properties have been described (e.g., oral dermal toxicity; danger skin corrosion/irritation). Thus, taking into account these properties and the results here described, nHo is a base of choice to prepare IL MALDI matrices and particularly CHCA.nHo for LMW carbohydrate analysis.

Acknowledgements

The authors are grateful to the University of Buenos Aires (UBACyT 20020170100110BA), Consejo Nacional de Investigaciones Científicas y Técnicas (CONICET PIP 0072CO) and to the Agencia Nacional de Promoción Científica y Tecnológica (PICT 2016-0130) for the financial support. TSDL developed this work with a fellowship from the ANPCyT and currently from CONICET. MLS and REB are Research Members of CONICET (Argentina). The Ultraflex II (Bruker) TOF/TOF mass spectrometer was supported by a grant from ANPCYT, PME 125.

Appendix A. Supplementary data

Supplementary data associated with this article, Scheme 1, Table S1, and Figures S1-S11, can be found, in the online version, at http://.....

References

[1] R.C. Beavis, T. Chaudhary, B. T. Chait. α -Cyano-4hydroxycinnamic Acid as a Matrix for Matrix assisted Laser Desorption Mass-Spectrometry. *Org. Mass Spectrom.* **1992**, *27*, 156.

[2] T.W. Jaskolla, W.D. Lehmann, M. Karas. 4-Chloro-α-cyanocinnamic acid is an advanced, rationally designed MALDI matrix. P.N.A.S. USA **2008**, *105*, 12200.

[3] T. Porta, C. Grivet, R. Knochenmuss, E. Varesioa, G. Hopfgartner. Alternative CHCA-based matrices for the analysis of low molecular weight compounds by UV-MALDI-tandem mass spectrometry. *J. Mass Spectrom.* **2011,** *46*, 144.

[4] U. Bahr, T.W. Jaskolla. Employing 'Second Generation' Matrices in R. Cramer (ed), Advances in MALDI and Laser-Induced Soft Ionization Mass Spectrometry, Springer, Switzerland. **2016**. pp 3-35.

[5] D.W. Armstrong, L.K. Zhang, L. He, M.L. Gross. Ionic liquids as matrixes for matrix-assisted laser desorption/ionization mass spectrometry. *Anal. Chem.* **2001**, *73*, 3679.

[6] A. Tholey, E. Heinzle. Ionic (liquid) matrices for matrix-assisted laser desorption/ionization mass spectrometry—applications and perspectives. *Anal. Bioanal. Chem*. **2006**, *386*, 24.

[7] J.A. Crank, D.W. Armstrong. Towards a Second Generation of Ionic Liquid Matrices (ILMs) for MALDI-MS of Peptides, Proteins, and Carbohydrates. *J. Am. Soc. Mass Spectrom.* **2009**, *20*, 1790.

[8] H. Nonami, S. Fukui, R. Erra-Balsells. β-Carboline Alkaloids as Matrices for Matrix-assisted Ultraviolet Laser Desorption Time-of flight Mass Spectrometry of Proteins and Sulfated Oligosaccharides: A Comparative Study Using Phenylcarbonyl Compounds, Carbazoles and Classical Matrices. *J. Mass Spectrom.* **1997**, *32*, 287.

[9] H. Nonami, K. Tanaka, Y. Fukuyama, R. Erra-Balsells. β-Carboline Alkaloids as Matrices for UV-Matrix-assisted Laser Desorption/Ionization Time-of-flight Mass Spectrometry in Positive and Negative Ion Modes. Analysis of Proteins of High Molecular Mass, and of Cyclic and Acyclic Oligosaccharides. *Rapid Commun. Mass Spectrom.* **1998**, *12*, 285.

[10] M.E. Monge, R.M. Negri, A.A. Kolender, R. Erra-Balsells. Structural characterization of native Highly-Methoxylated Pectin using UV-MALDI-TOF Mass Spectrometry. Comparative use of 2,5-dihydroxybenzoic acid and nor-harmane as UV-MALDI matrices. *Rapid Commun. Mass Spectrom.* **2007**, *21*, 2638.

[11] M. Ciancia, Y. Sato, H. Nonami, A.S. Cerezo, R. Erra-Balsells, M.C. Matulewicz. Autohydrolysis of a partially cyclized mu/nu-carrageenan and structural elucidation of the oligosaccharides by chemical analysis, NMR spectroscopy and UV-MALDI mass spectrometry. *ARKIVOC* **2005**, *XII*, 319.

[12] M. Barboza, V.G. Duschak, Y. Fukumaya, H. Nonami, R. Erra-Balsells, J.J. Cazzulo, S. Couto. Structural Analysis of the N-glycans present in the C-terminal domain of the major cysteine proteinase of *Trypanosoma cruzi*. Identification of sulfated high-mannose type oligosaccharides. *FEBS Journal* **2005**, *272*, 3803.

[13] M. Landoni, V.G. Duschak, V.J. Peres, H. Nonami, R. Erra-Balsells, A.M. Katzin, A.S. Couto. *Plasmodium falciparum* biosynthesizes sulfoglycosphingolipids. *Mol. Biochem. Parasitol.* **2007**, *154*, 22.

[14] A.C. Casabuono, A. D'Antuono, Y.Sato, H. Nonami, R. Ugalde, V. Lepek, R. Erra-Balsells, A.S. Couto. A matrix-assisted Laser desorption/ionization mass spectrometry approach of the Lipid A from *Mesorhizobium loti*. *Rapid. Commun. Mass Spectrom.* **2006**, *20*, 2175.

[15] R. Erra-Balsells, H. Nonami. Nor-Harmane (9H-Pyrido[3,4-b]indole) as Outstanding Matrix for UV-Matrix-assisted Laser Desorption/Ionization Time-of-flight Mass Spectrometry Analysis of Synthetic and BioPolymers. *Environ. Control in Biology* **2002**, *40*, 55.

[16] E.M. Rustoy, Y. Sato, H. Nonami, R. Erra-Balsells, A. Baldessari. Lipase-Catalyzed Synthesis and Characterization of Copolymers from Ethyl Acrylate as the Only Monomer Starting Material. *Polymers* **2007**, *48*, 1517.

[17] M.R.L. Paine, B.L.J. Poad, G.B. Eijkel, D.L. Marshall, S.J. Blanksby, R.M.A. Heeren, S.R. Ellis. Mass Spectrometry Imaging with Isomeric Resolution Enabled by Ozone-Induced Dissociation. *Angew. Chem. Int. Ed.* **2018,** *57*, 10530.

[18] F.P.Y. Barré, B.S.R. Claes, F. Dewez, C. Peutz-Kootstra, H.F. Munch-Petersen, K. Grønbæk, A. H. Lund, R.M.A. Heeren, C. Côme, B. Cillero-Pastor. Specific Lipid and Metabolic Profiles of R-CHOP-Resistant Diffuse Large B-Cell Lymphoma Elucidated by Matrix-Assisted Laser Desorption Ionization Mass Spectrometry Imaging and in Vivo Imaging. *Anal. Chem.* **2018**, *90*, 14198.

[19] M.C. Biondic, R. Erra-Balsells. Photochemical Reaction of β-Carbolines in Carbon Tetrachloride-Ethanol mixtures. *J. Photochem. Photobiol. A: Chem.* **1990**, *51*, 341.

[20] F.T. Vert, I.Z. Sanchez, A.O. Torrent. Acidity constants of β-carbolines in the ground and excited singlet states. *J. Photochem.* **1983**, *23*, 355.

[21] Y. Gholipour, H. Nonami, R. Erra-Balsells. In Situ Analysis of Plant Tissue Underivatized Carbohydrates and On-Probe Enzymatic Degraded Starch by Matrix-Assisted Laser Desorption/Ionization Time-of-Flight Mass Spectrometry by using Carbon Nanotubes as Matrix. *Anal. Biochem.* **2008**, *383*, 159.

[22] Y. Gholipour, S.L. Giudicessi, H. Nonami, R. Erra-Balsells. Diamond, Titamiun Dioxide, Strontium Titanium Oxide, and Barium Strontium Titanium Oxide Nanoparticles for Direct Matrix Assisted Laser Desorption/Ionization Mass Spectrometry Analysis of Soluble Carbohydrates in Plant Tissues. *Anal. Chem.* **2010**, *82*, 5518.

[23] D.J. Harvey. Matrix-assisted laser desorption/ionization mass spectrometry of carbohydrates. *Mass Spectrom. Rev.* **1999**, *18*, 349.

[24] C.D. Calvano, A. Monopoli, T.R.I. Cataldi, F. Palmisano. MALDI matrices for low molecular weight compounds: an endless story? *Anal. Bioanal. Chem.* **2018**, *410*, 4015.

[25] D.J. Harvey. Analysis of carbohydrates and glycoconjugates by matrix-assisted laser desorption/ionization mass spectrometry: an update covering the period 2007-2008. *Mass Spectrom. Rev.* **2012**, *31*, 183.

[26] Y. Dai, R.M. Whittal, C.A. Bridges, Y. Isogai, O. Hindsgaul, L. Li. Matrix-assisted laser desorption ionization mass spectrometry for the analysis of monosulfated oligosaccharides. *Carbohydr. Res.* **1997**, *304*, 1.

[27] Y. Fukuyama, S. Nakaya, Y. Yamazaki, K. Tanaka. Ionic liquid matrixes optimized for MALDI-MS of sulfated/sialylated/neutral oligosaccharides and glycopeptides. *Anal. Chem.* **2008**, *80*, 2171.

[28] Y. Fukuyama, M. Ciancia, R. Erra-Balsells, M.C. Matulewicz, H. Nonami, A.S. Cerezo. Matrix-assisted ultraviolet laser desorption ionization time-of-flight mass spectrometry of sulfated carrageenan oligosaccharides. *Carbohydr. Res.* **2002**, *337*, 1553.

[29] M.W. Towers, J.E. McKendrick, R. Cramer. Introduction of 4-chloro-α-cyanocinnamic acid liquid matrices for high sensitivity UV-MALDI MS. *J. Proteome Res.* **2010**, *9*, 1931.

[30] M.W. Towers, R. Cramer. Ionic Liquids and Other Liquid Matrices for Sensitive MALDI MS Analysis in R. Cramer (ed), Advances in MALDI and Laser-Induced Soft Ionization Mass Spectrometry, Springer, Switzerland. **2016,** pp. 50-64.

[31] O.I. Tarzi, H. Nonami, R. Erra-Balsells. Temperature effect on the stability of compounds used as UV-MALDI-MS matrix: 2,5-Dihydroxybenzoic acid, 2,4,6-Trihydroxyacetophenone, trans-α-Cyano-4-hydroxycinnamic acid, 3,5-Dimethoxy-4-hydroxycinnamic acid, nor-Harmane and Harmane. *J. Mass Spectrom.* **2009**, 44, 260.

[32] R. Erra-Balsells, A.R. Frasca. Photochemical Dimerization of β-Carboline Alkaloids. *Tetrahedron* **1983**, 39, 33.

[33] M. Klessinger, J. Michl. Excited States and Photochemistry of Organic Molecules; VCH Publishers, Inc., New York, **1995**, pp. 362;

[34] N.J. Turro, V. Ramamurthy, J.C. Scaiano. Principles of Molecular Photochemistry: An Introduction. University Science Books, Sausalito **2009**. pp. 319.

[35] M.L. Salum, P. Arroyo-Manez, F.J. Luque, R. Erra-Balsells. A Combined Experimental and Computational Investigation of the Absorption Spectra of *E*- and *Z*-Cinnamic Acids in Aqueous Media: The peculiarity of Z-Cinnamics, *J. Photochem. Photoiol. B: Biology* **2015**, *148*, 128.

[36] B. Stahl, M. Steup, M. Karas, F. Hillenkamp. Analysis of neutral oligosaccharides by matrix-assisted laser desorption/ionization mass spectrometry. *Anal. Chem.* **1991**, *63*, 1463.

Table 1. Dynamic range and limit of detection of bCD in the positive ion mode, and of NCT in the negative ion mode using different matrices[a] .

Matrix	bCD [b]		NCT [c]	
	LOD	Dynamic Range	LOD	Dynamic Range
nHo	2.59	2.59-2590.00	2.59	2.59-2590.00
CHCA	5.15	5.15-515.00	5.15	5.15-515.00
CHCA.BAM	2.59	2.59-2590.00	2.59	2.59-2590.00
CHCA.nHo	0.51	0.51-2590.00	0.51	0.51-2590.00

[a] LOD, limit of detection. indicatted as pmol of carbohydrate deposited on the probe; S/N ≥ 4.
[b] Positive ion mode; β-cyclodextrin: bCD;. monitoring ion $[M+Na]^+$
[c] Negative ion mode; neocarratetraose $4^1,4^3$-disulfate disodium salt: NCT; monitoring ion $[M-Na]^-$

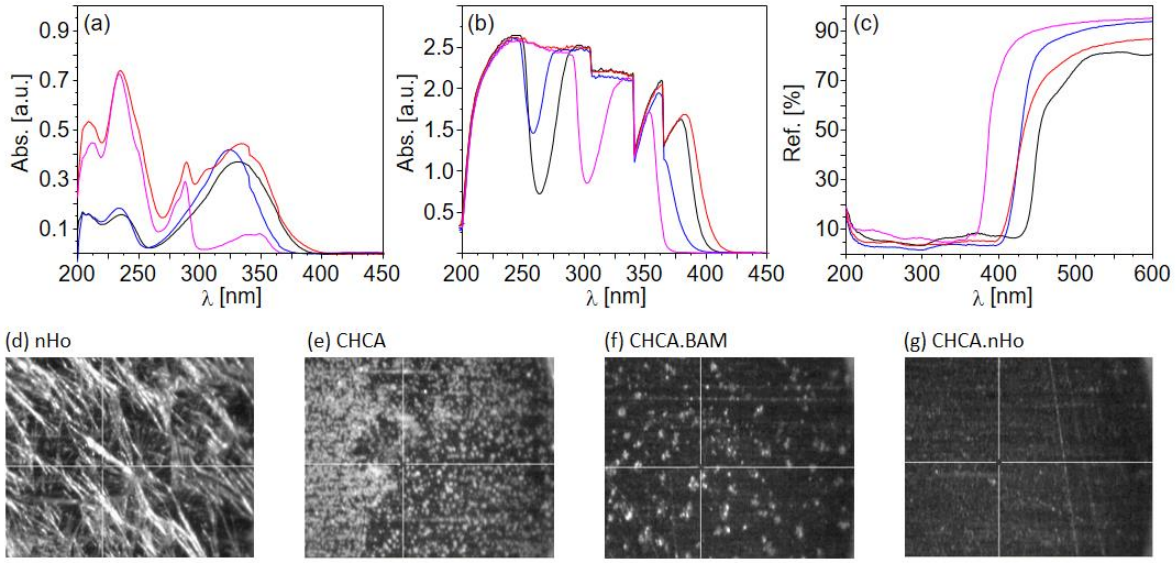

Figure 1. Top: UV-visible absorption spectra in solution. Solvent: methanol. Concentration: (a) 2x10-5 M and (b) 1x10-3 M. UV-visible diffuse reflectance spectra, solid sample (c). Analytes: nHo (pink), CHCA (black), CHC.BAM (blue) and CHCA.nHo (red). Bottom: Optical image of solid matrix on the MALDI probe: (d) nHo, (e) CHCA, (f) CHCA.BAM and (g) CHCA.nHo. Center of the spot.

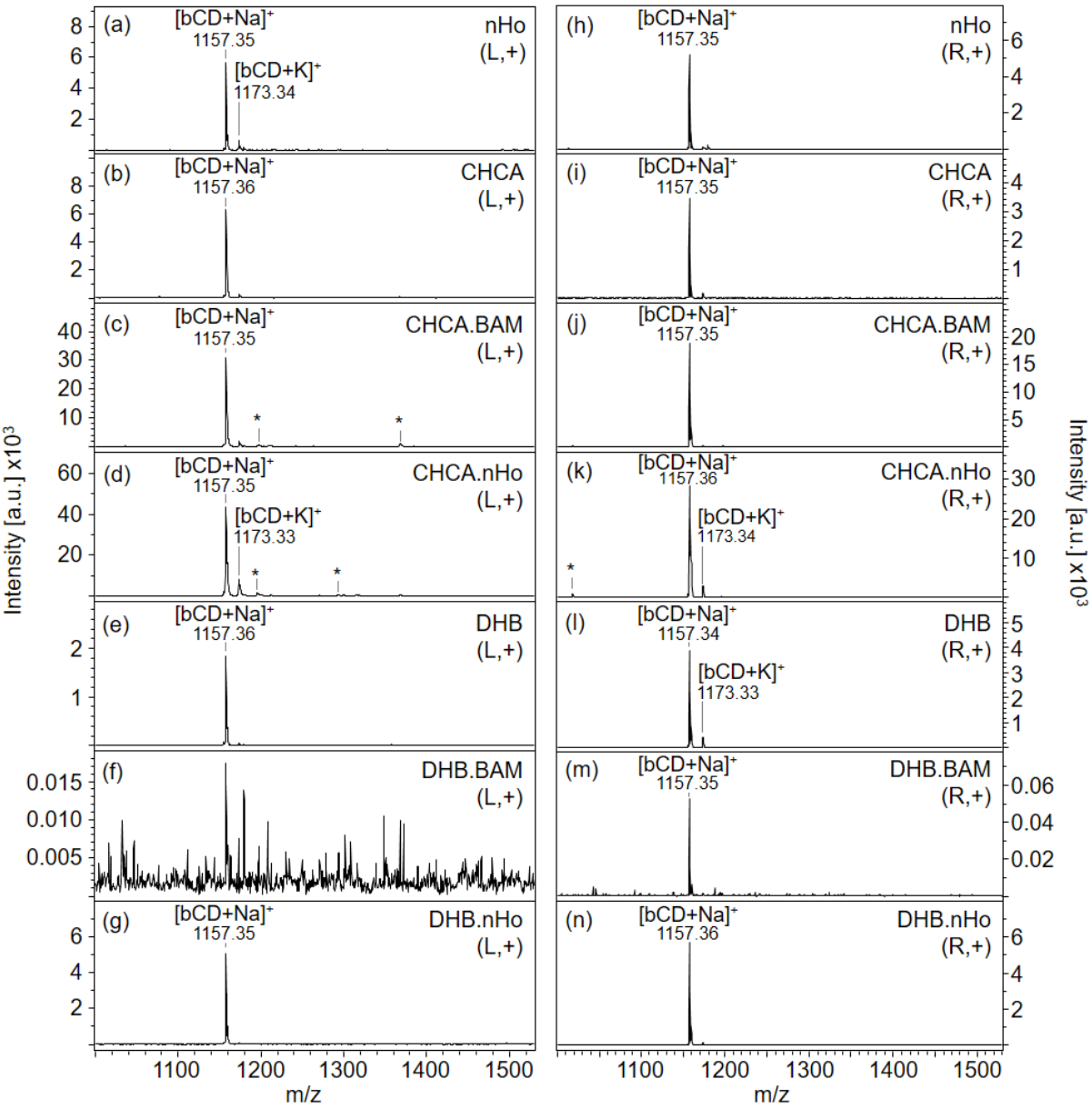

Figure 2. MALDI mass spectra. Analyte: bCD. Matrix, linear mode (L): (a) nHo, (b) CHCA, (c) CHCA.BAM, (d) CHCA.nHo, (e) DHB, (f) DHB.BAM and (g) DHB.nHo. Matrix, Reflectron mode (R): (h) nHo, (i) CHCA, (j) CHCA.BAM, (k) CHCA.nHo, (l) DHB, (m) DHB.BAM and (n) DHB.nHo. Positive ion mode (+). * No assigned cluster. Laser power 20%.

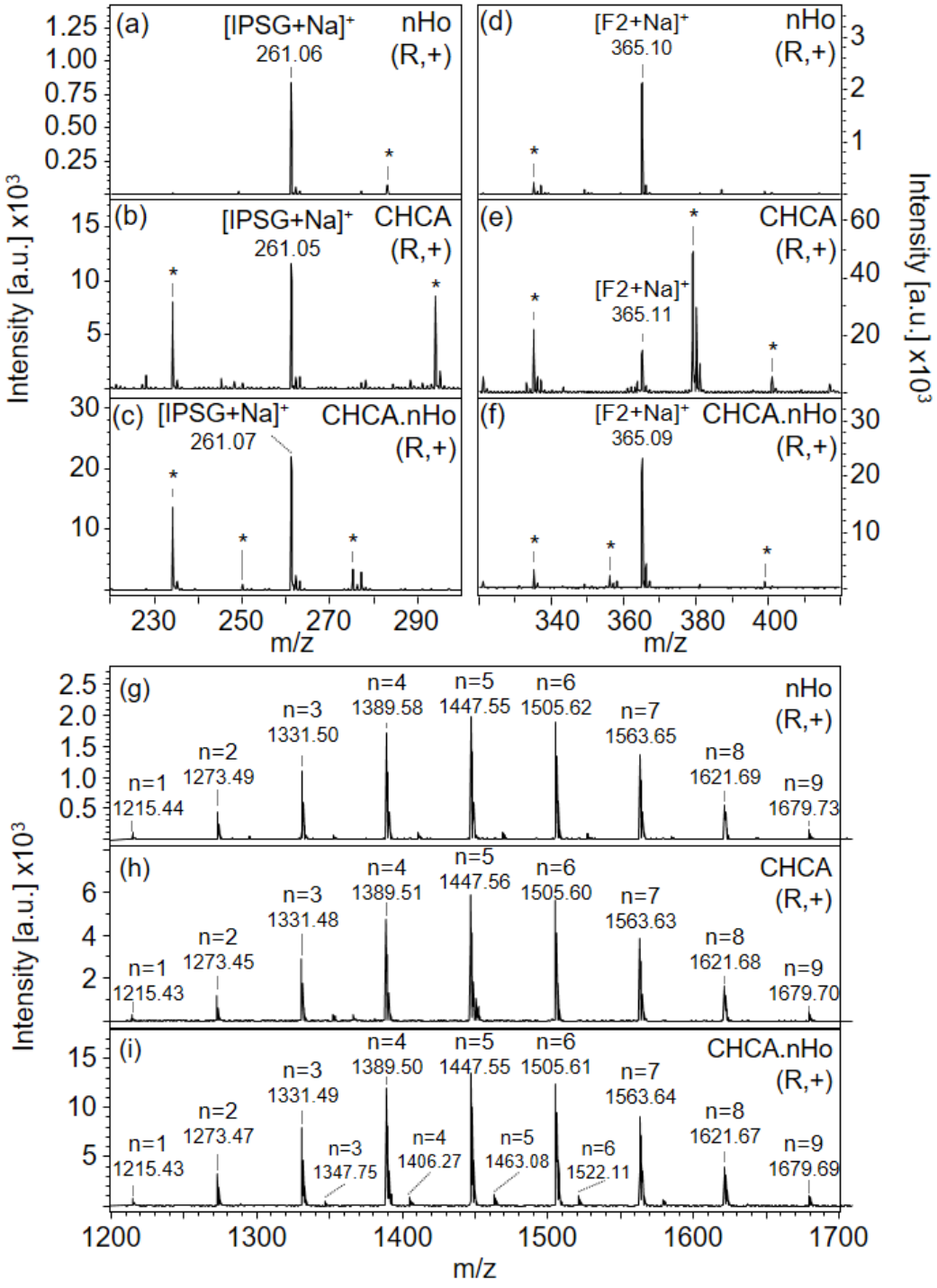

Figure 3. MALDI mass spectra. Analyte: IPSG (top left column, a-c), F2 (top right column, d-f), (HOP)nbCD (bottom, g-i). Matrix: nHo (a, d, g), CHCA (b, e, h), CHCA.nHo (c, f, i). Reflectron positive ion mode (R,+). (HOP)nbCD = (HOP)1-9bCD, e.g., [(HOP)5bCD+Na] = 1447 m/z and [(HOP)5bCD+K] = 1463 m/z. Laser power 20%.

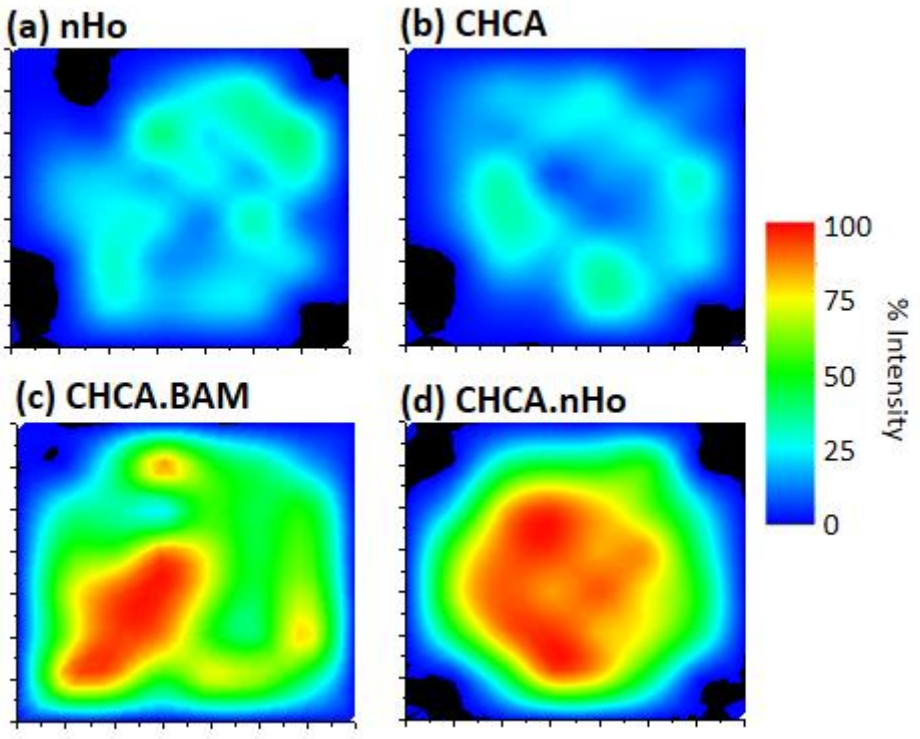

Figure 4. Spot surface intensity maps. Monitoring ion: [M+Na]+. Analyte: bCD. Matrix: (a) nHo, (b) CHCA, (c) CHCA.BAM and (d) CHCA.nHo. Positive ion mode. Normalized intensity scale: Lower in blue and maximum in red. Laser power 20%.

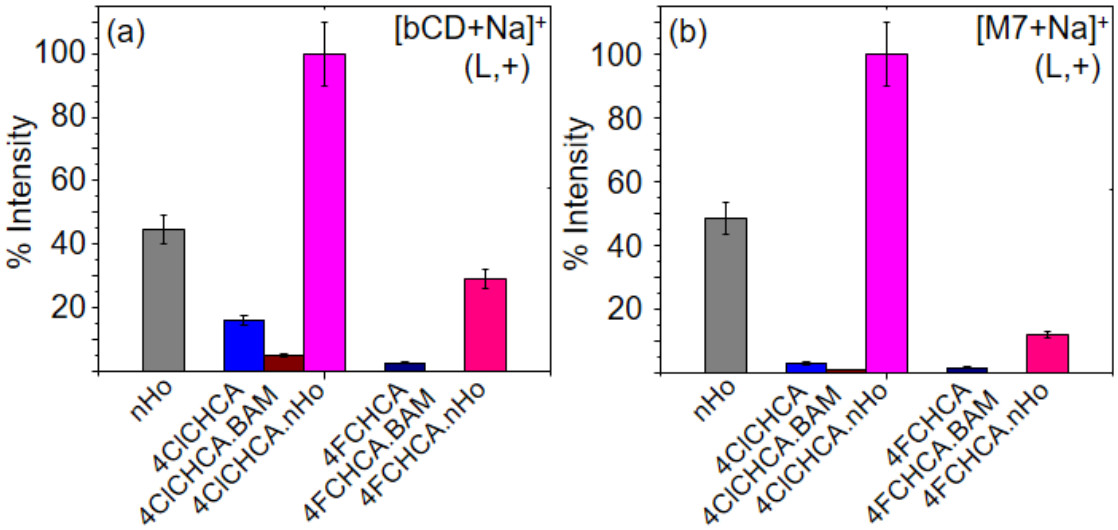

Figure 5. The levels of differences of [M+Na]+ ions between the same neutral carbohydrate analyzed with different crystalline matrix and IL matrix. The "y"-axis represents the normalized peak intensity; matrix are indicated in the "x"-axis. Carbohydrate: (a) bCD (left) and (b) M7 (right). Linear positive ion mode (L,+). Laser power 20%.

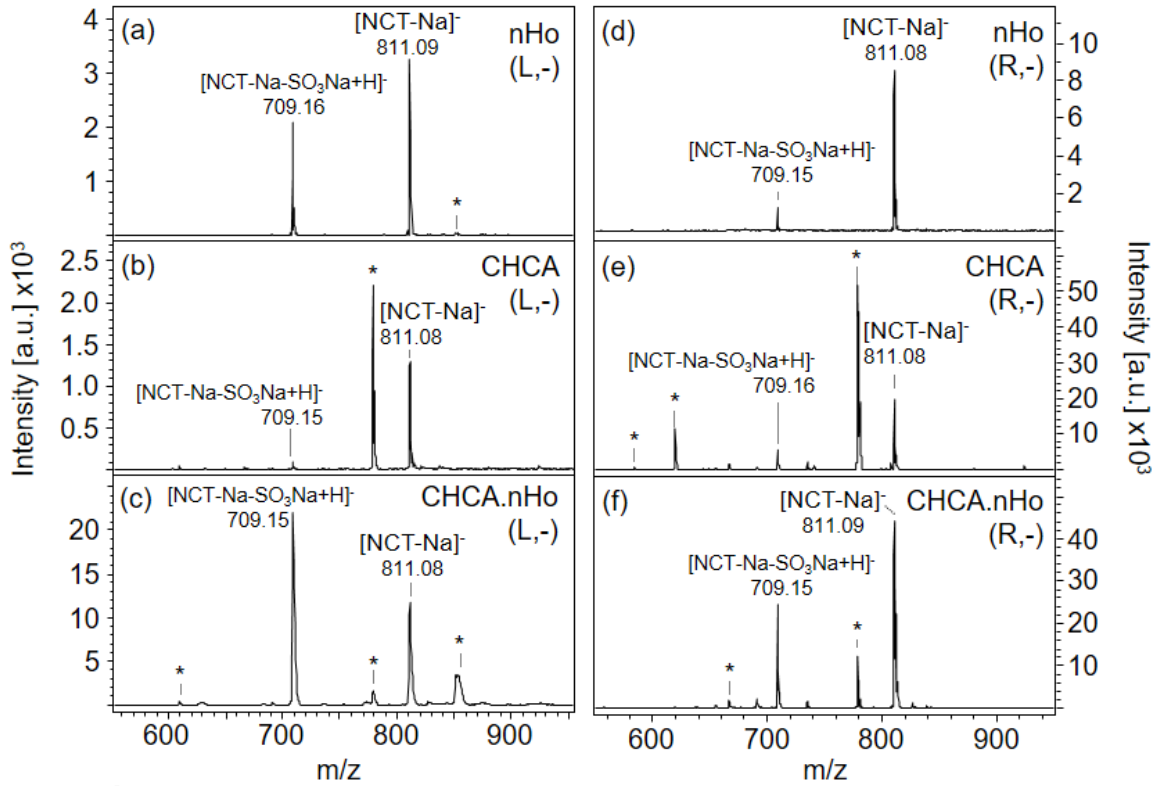

Figure 6. MALDI mass spectra. Analyte: NCT. Matrix, linear mode (L): (a) nHo, (b) CHCA and (c) CHCA.nHo; Matrix, reflectron mode (R): (d) nHo, (e) CHCA and (f) CHCA.nHo. Negative ion mode (-). Laser power 20%.

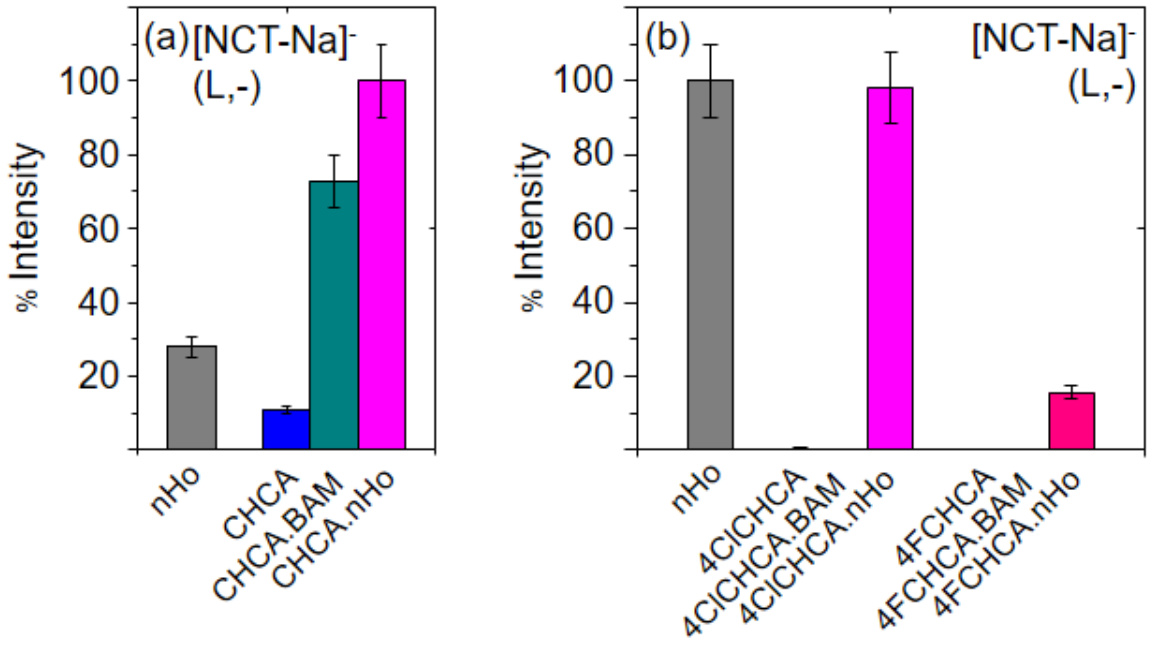

Figure 7. The levels of differences of [M-Na]- ions between the same sulfated carbohydrate analyzed with different crystalline matrix and IL matrix. The "y"-axis represents the normalized peak intensity; matrix are indicated in the "x"-axis. Carbohydrate: NCT. (a) laser power 20% and (b) laser power 40 %. Linear negative ion mode (L,-).